Tech Science Press

Hybrid Microgrid based on PID Controller with the Modified Particle Swarm Optimization

R. K. Rojin[1,*] and M. Mary Linda[2]

[1]Sivaji College of Engineering and Technology, Anna University, Chennai, 600025, India
[2]Ponjesly College of Engineering, Anna University, Chennai, 600025, India
*Corresponding Author: R. K. Rojin. Email: rkrojin123@gmail.com

Abstract: Microgrids (MG) are distribution networks encompassing distributed energy sources. As it obtains the power from these resources, few problems such as instability along with Steady-State (SS) issues are noticed. To address the stability issues, that arise due to disturbances of low magnitude. Small-Signals Stability (SSS) becomes mandatory in the network. Convergence at local optimum is one of the major issues noticed with the existing optimization algorithms. This paper proposes a detailed model of SSS in Direct Current (DC)-Alternate Current (AC) Hybrid MG (HMG) using Proportional Integral and Derivative Controller (PIDC) tuned with Modified Particle Swarm Optimization (MPSO) algorithm to alleviate such issues. The power is extracted from Renewable Energy Resources (RER), such as Photovoltaic (PV), Micro-Hydro (MH), and Wind Energy Conversation System (WECS). For tracking the power more efficiently, Maximum Power Point Tracking (MPPT) techniques are employed. Boost Converters (BC) are used and inverters are employed to convert DC to the AC. Here, the power flow is managed by the PIDC. If the Firing Angle (FA) is not properly determined, it results in instability and steady-state stability issues. To address this, the optimum tuning parameters are chosen for PIDC, by utilizing the MPSO. Finally, through experimentation analysis, the proposed system's performance is analyzed and compared with the existing algorithms and validated.

1 Introduction

MG is the constituent of smart grid technologies, and it can ameliorate the Power System's (PS) economics, resilience, security, reliability, along with sustainability [1]. The MG demand is augmented on account of the MG's benefits [2]. An MG is typically split into three categories: AC-MG, DC-MG, and hybrid AC/DC-MG can familiarize as a small-PS, that facilitates the larger-scale RER's integration along with the application [3]. HMG has more advantages, better power-sharing, enhanced system dynamics, and optimum management than the other MG's [4]. Recently, RES have been extensively adopted in electric

grids [5]. More integration of RES is encouraged by the beneficial traits of the MG conception. In addition, ancillary services concerning frequency support together with voltage regulation could well be potentially commenced by MG [6]. Wind Generation (WG), Fuel Cells (FC), PV, micro-turbines, and hydropower turbines are the main RER that demands hybrid AC/DC-MG, and generates intermittent output power [7,8].

Though RES has countless advantages, the MG under RES suffers from dynamic performance issues along with stability [9]. The stability issues can well be mostly split into the SSS and the larger disturbance stability, as per the disturbance nature [10]. In a MG, the SSS [11] is associated with the feedback controller, increased load switching, along with the power limit of micro-sources. A fault with a succeeding island poses greater disturbance stability issues. Amongst the assortment of stability issues, encompassing poor SSS [12] will be a concern for attaining the dependable function of the MG. In addition, SS stability issues are as well found in the HMG. The stability issue is labelled as the instability that relies on DG units intended for sufficient balancing of energy [13]. The control system adopted finds the solution for instability issues [14].

In the MG, two sorts of control strategies were employed. The second control approach applies a completely decentralized method signifying locally controlled units [15]. Numerous control techniques as Proportional-Integral (PI) controller [16], PIDC [17], as well as a fuzzy logic controller [18], are proposed in various literatures. If the controllers are not fed with the optimum parameters, instability issues remain, hence as a result, the optimal selection is required. Nevertheless, many techniques encounter slower convergence speed together with erroneous outcomes [19]. Lately, nature-inspired algorithms are turning out to be an attractive solution for minimizing or maximizing non-differentiable non-linear function, say Genetic Algorithm (GA) [20] Particle Swarms Optimization (PSO) [21], however, undergo premature convergence.

2 Literature Survey

Shahsavari et al. [22] rendered a mathematical strategy for examining the high infiltration effects induced by the PV power plant on the SSS of a power network and for ameliorating the probabilistic SSS of the PS, utilizing the optimal Fractional Order (FO) PIDC. In this strategy, a Non-dominated Sorting GA (NSGA-II) type multi-objective optimization approach was employed for ascertaining the FO-PID stabilizer-centric parameters on the basis of two performance indices, such as Integral Square Error (ISE) and Integral Absolute Error (IAE).

Ray et al. [23] recommended frequency control in MG consisting of wind, diesel engine generators, PV, and fuel cell accompanied by the energy storage (ES), as battery ES and flywheel ES. A firefly-integrated particle swarm (FF-PSO) centric hybridized optimization structure was utilized for tuning parameters, and the PIDC was utilized for lessening the frequency deviation in the MG structure under diverse operating scenarios, like the variations in load demand and wind speed (WS).

Abdulkhader et al. [24] examined some impacts of Renewable Energy (RE) System-centered MG penetration on the control and dynamic stability of an effective multi-area multi-machine structure under diverse operating scenarios. The model of a type-2 fuzzy FOPID-centric PS stabilizer (PSS), by introducing a meta-heuristic hybridized algorithm for enhancing the stability.

Nezhadpashaki et al. [25] built a dynamic strategy for Inverter Based Distribution Generation units (IBDG), loads, and network branches. This strategy scrutinized some impacts of SSS constraint on optimum location, accompanied by the IBDG's size in a radial distribution framework. GA was utilized to ascertain the IBDG's optimal size and optimal location for reducing the total active power loss. Propounded an adaptive fuzzy proportional-integral controller [26] for ameliorating the dynamic performance, rendered by the inverter interfaced autonomous MG. The propounded model had the controller dynamics, network dynamics, load dynamics, and dynamics of a filter. Renuka et al. [27]

developed PSO methodology, a multi-stage optimization approach, for ameliorating the SSS and energy penetration. The work had two stages: initially, the PSO was employed for maximizing RE penetration to the test structures. Secondly, the system's SSS was ameliorated with maximal RE penetration.

Santhoshkumar et al. [28] recommended the transient along with SSS enhancement in MG, employing Whale Optimization Algorithms (WOA) together with Ant Lion Optimization (AWOALO) and virtual Synchronous Generators (SG). AWOALO was executed to regulate optimally the parameters, thus ensure a smooth transition, subsequent to an alteration or disturbance. Yi Zhang et al. [29] established an adaptive coordinated control approach aimed at the networked AC/DC MG, for ameliorating the system's frequency along with DC voltage stability. Initially, the converter strategy was designed, based on the synchronverter and virtual DC machine. Further, to ameliorate the system stability's performance, the parameter model of the Adaptive Virtual Inertia (AVI) together with virtual Governor-Gain (GG) was employed consequently. To address the stability issues that arise due to disturbances of low magnitude Small-Signals Stability (SSS) becomes mandatory. Convergence at local optimum is one of the major issues noticed with the existing optimization algorithms. This paper proposes a detailed model of SSS in Direct Current-Alternate Current Hybrid MG using Proportional Integral and Derivative Controller tuned with Modified Particle Swarm Optimization (MPSO) algorithm to alleviate such issues.

3 Enhancement of Small Signal Stability in DC-AC Hybrid Microgrid Based On PID Controller with MPSO Algorithm

Currently, MG has undergone quick development, as it is proved to be an effectual solution for the dependable hybridization of Distributed Generations (DG) units, energy storage systems, along with loads, that functions in grid-connected or islanded mode. Here, the HMG has the competency to be joined directly to the major power grid. In the hybrid grid, the power is supplied to the Dynamic Load (DL) or static load. Most researches analyze the stability in static loads, intended for an MG. DL considerably influences the MG's stability on account of its voltage along with frequency-dependent nature. Thus, a smaller variation in voltage together with frequency can make a considerable effect on the MG's stability with the existence of DL. In the proposed work, the power is produced as the combination of RES, say, PV, WECS, along with MH, which is supplied to the DL in the HMG. BC is used for a grid-linked HMG, the current being managed by FA control. Further, the PIDC is employed for controlling the FA to avoid the stability issues. To overcome the stability issue and to enhance SSS, MPSO is employed for optimizing the parameters and is aimed at designing the perfect controller that renders the better outcome. The block diagram is of the proposed system is given in Fig. 1.
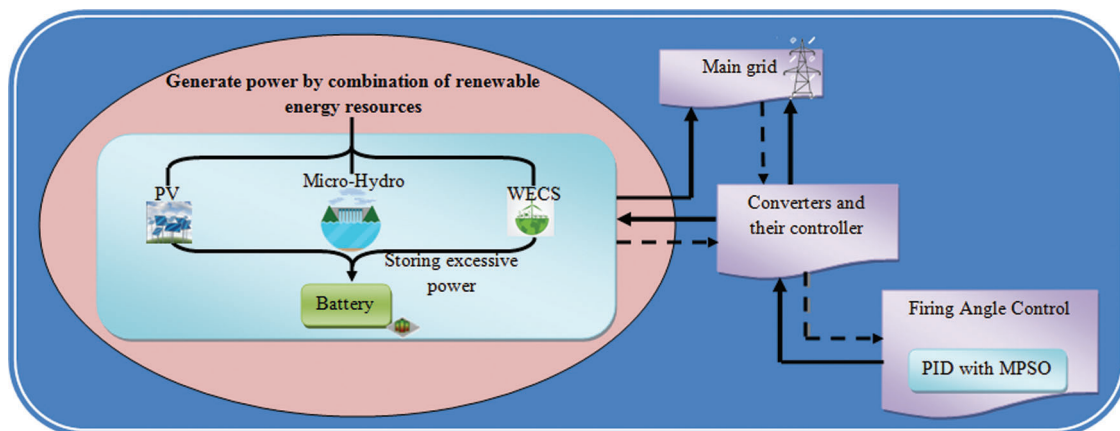

Figure 1: Block diagram for the proposed methodology

3.1 Renewable Energy Resources

Initially, the combination of RER, say PV, MH, and WECS, is employed for producing power. In RES, the MPPT is employed to achieve maximum power extraction in the entire conditions. In addition, when the load is higher, analogized to the particular threshold, the remaining power is stored on the battery.

3.1.1 PV Modeling

Utilizing PV modules, the solar energy is changed to electricity. The solar cells can be joined in parallel or series, relying on the preferred voltage as well as current [30]. The output current power (C) is stated as,

$$C = C_{pc} - C_o \left[e^{\frac{g(S_r)}{M_B Temp\ \alpha}} - 1 \right] - \frac{(vol + S_r)}{S_p} \tag{1}$$

wherein, g implies the charge of the electron, C_o signifies the saturation current, S_r and S_p implies the series and parallel resistances, α signifies the ideality factor, $Temp$ signifies the actual temperature, vol implies the voltage, M_B implies the Boltzmann constant, together with C_{pc} implies the photocurrent. The photocurrent counts on the variation of the radiance along with temperature as,

$$C_{pc} = \left[C_{sc} + k_{co} \left(Temp - Temp_{ref} \right) \right] \chi \tag{2}$$

Wherein, C_{sc} implies the short-circuit current, $Temp_{ref}$ signifies the reference temperature, k_{co} signifies the co-efficient of temperature at C_{sc} along with χ signifies the radiance value in kW/m^2, therefore, the expression of the current rendered by means of the PV Array (PVA) is given in the succeeding equation:

$$C = A_p C_{pc} - A_p C_o \left[e^{\frac{vol + C(A_S A_P)S_r}{A_s \alpha Vol_{th}}} - 1 \right] - \frac{vol + C\left(\frac{A_s}{A_p}\right) S_r}{\left(\frac{A_s}{A_p}\right) S_p} \tag{3}$$

Wherein, A_s signifies the total modules in series and A_p implies the total modules in parallel together with Vol_{th} imply the total voltage.

3.1.2 Micro-Hydro Modeling

The power that is produced, as of a MH power plant relies on the head's size along with hydro discharge [31]. MH potential energy (P_e) is computed based on the following equation:

$$P_e = h_m . j_l . w_f \tag{4}$$

Wherein, h_m implies the hydro mass (kg), w_f signifies the waterfall (m), and j_l implies the gravitational constant $\left(m/s^2\right)$.

Hydro-potential aimed at electrical energy can be attained, as of a lower hydro-flow. The energy generated is kinetic and given, as per the subsequent equation:

$$P_e = \frac{1}{2} h_m \upsilon^2 \tag{5}$$

Wherein, h_m implies the hydro mass (kg) together with υ signifies hydro-flow velocity (m/s).

Therefore, the electrical power produced by the MH plant (μ) can be computed as per the subsequent equation:

$$\mu = \frac{1}{2} h_d X_a v^3 \tag{6}$$

Wherein, h_d implies the hydro density (kg/m^3), X_a signifies a cross-sectional region of hydro flow (m^2), along with v implies hydro flow velocity (m/s).

3.1.3 WECS Modeling

The power output as of the wind counts on the WS, which is computed based on the power-law equation, as rendered in the subsequent equation:

$$E = E_0 \left(\frac{F}{F_0}\right)^x \tag{7}$$

Wherein, E and E_0 imply the WS at the hub and reference height F and F_0 and x implies the power-laws exponent. The power of the Wind Turbines (WT) $(Y_w(kW/m^2))$ is illustrated concerning the WS by,

$$\begin{cases} 0 & E_{cut-in}, E > E_{cut-off} \\ Y_{WG-\max} \times ((E - E_{cut-in})/(E_{rated} - E_{cut-in}))^3 & E_{cut-in} \leq E < E_{rated} \\ Y_{WG-\max} \times \dfrac{Y_{furl} - Y_{rated}}{E_{cut-off} - E_{rated}} \times (E - E_{rated}) & E_{rated} \leq E \leq E_{cut-off} \end{cases} \tag{8}$$

Wherein, E_{cut-in} signifies cut-in WS $[m/s]$, $E_{cut-off}$ implies cut out WS $[m/s]$, E signifies wind speed $[m/s]$, E_{rated} implies nominal WS $[m/s]$, E_{rated} signifies nominal power of WT $[kW]$, $Y_{WG-\max}$ signifies maximum power of WT $[kW]$, along with Y_{furl} implies power of WT in cut-out WS $[kW]$. The actual power available as of a WT (i.e., Y) is rendered by,

$$Y = Y_W(t) \, SS_W \, \beta \, N_{WG} \tag{9}$$

Wherein, $Y_W(t)$ implies the WT's power at time t, SS_W signifies swept area, β implies the effectiveness of the WT generator and equivalent converters, and N_{WG} implies the number of WT generators at site.

3.1.4 Battery Modeling

Subsequent to power gain, as one of the complete resource, the battery stack is employed to store the energy, as the produced power is more compared to the load demand. As the generation can't fulfil the load needs, the battery power will be extracted. Relying on the charging along with discharging state, the current may be negative or positive.

$$ST_g = C + \mu + Y - AD_l \tag{10}$$

In which ST_g implies the battery, along with AD_l signifies the hybrid DC and AC-DL, subsequent to AC and DC load, the remaining power is stored in the battery. Here, a DL profile is given, where the needed power has the behavior of a controlled current source, wherein load power is equivalent to

$$AD_{load} = C_{load} \cdot Vol_{bus} \tag{11}$$

Wherein, AD_{load} implies the ac and dc loads, C_{load} signifies the current load, and Vol_{bus} implies the voltage bus.

Fig. 2 shows the proposed DC-AC HMG's design. The power is transported to the main grid, utilizing the converters. MH, WECS, and the AC loads are connected to the AC bus; the battery, PV along with DC loads is connected to the DC bus.
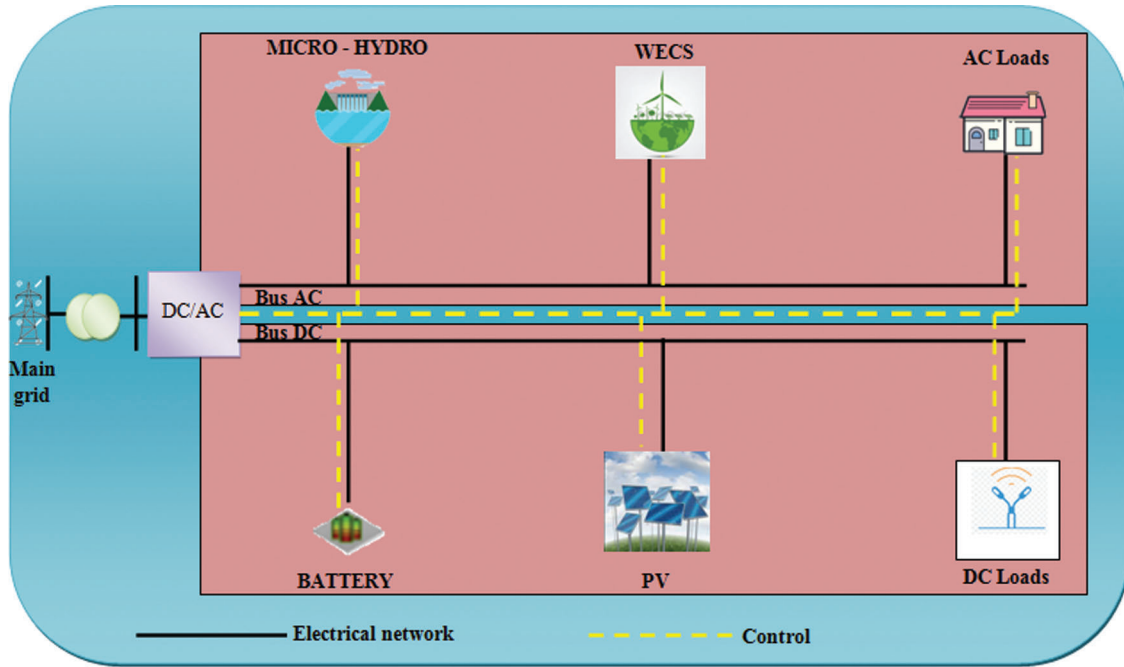
Figure 2: DC-AC HMG structure

3.2 Converters and Their Controllers

The attained power as of RER is fed to the MG, utilizing the BC with PIDC. The BC is utilized in the proposed technique. The current is managed by FA. Thus, FA is a significant measure. If it exceeds the particular angle, SSS issue and the SS stability issue are raised in the converter. Therefore, the FA is ought to be controlled, by utilizing the PIDC. In PIDC, the input parameter is chosen by means of the MPSO, and discussed in the sections below.

PID controller: In PIDC, the proportional gain output is large, as the errors are larger. In the case of Integral, the error will be added continuously, as well as multiply with a constant. The derivative path's output signal is rendered by means of the Rates of Change (ROC) of error. The output is less, as the ROC of error is low, and larger as the ROC of error is high. PIDC will eradicate the forced oscillations along with SS error. The controller's output is mathematically written as,

$$C_t(\alpha_i(t)) = P_i \cdot \Delta\alpha_i(t) + I_i \int_0^t \Delta\alpha_i(t)dt + D_i \Delta\alpha_i(t) \tag{12}$$

Wherein, $\Delta\alpha_i(t)$ and $C_t(\alpha_i(t))$ implies the FA and controlled FA output, and also P_i, I_i, and D_i implies the proportional, integral, and also derivative parameters, correspondingly. Therefore, the preliminary parameters are chosen, utilizing the MPSO. PSO is basically a sort of swarm intelligence algorithm. It is influenced *via*, the collective behaviour of animals, explicitly, their food searching activities. When the PSO is employed to procure the optimum solution, the premature convergence happens, bringing about a local minimum. To evade this issue, the proposed system utilizes the MPSO. The initialized particle is mutated *via* the MPSO, prior to the updation of the particle's velocity. Generally, the mutation is performed arbitrarily. However, the mutation procedure is performed *via* computing Mahalanobis distance between the triumphant particle, that is kept in the starting point and the remaining particles, in successive. If the distance is higher analogized to the threshold, then the particle that has a higher threshold is mutated. It lessens the diversity together with convergence issue. MPSO begins with the

arbitrary initialization of a population of particles on the search space. Every individual in MPSO flies on the search space having a velocity, adjusted dynamically as per its own, together with its mate's flying knowledge. To attain optimum results, each particle shifts to its previous best ('pbest') position in conjunction with the global best ('gbest') position on the swarm. The expression of the p best together with the gbest is exhibited in the subsequent equation:

$$p_t(i, r) = \underset{r=1,\dots\dots,t}{\arg} \min[e(q_i(r))], \qquad i \in \{1, 2, \dots\dots, Z_p\} \tag{13}$$

$$g_t(r) = \underset{\substack{i=1,\dots\dots,Z_p \\ r=1,\dots\dots,r}}{\arg} \min[e(q_i(r))] \tag{14}$$

Wherein, i implies the particle index, Z_p signifies the total number of particles, r implies the present iteration number, $p_t(i, r)$ implies the pbest values, $g_t(r)$ illustrates the global best, e implies the Fitness Function (FF) and q ascertained the position. Next, the FF is computed. In the proposed system, the Integral of the Time-weighted Absolutes of the Error (ITAE) is regarded, which integrates the absolute error multiplied by average of the error over time. ITAE tuning makes the systems stay more swiftly than the other two tuning methods, namely ISE and IAE.

$$T_e = \int_0^\infty (t \cdot |e(t)|) \cdot dt \tag{15}$$

Wherein, t implies the time and T_e signifies the ITAE. The $e(t)$ states the error that is the difference between the input FA and the output SSS and SS error (*i.e.*, output), and it is expressed as,

$$e(t) = \alpha_i(t) - \Delta\alpha_i(t) \tag{16}$$

Wherein, $e(t)$ denotes the error, $\Delta\alpha_i(t)$ signifies the input, together with $\alpha_i(t)$ implies the output. Based on the error, integral performance criteria were developed in the control system. Subsequent to estimating the FF, the particle position is mutated. Arbitrary mutation renders the diversity issue, so that, initially, the standard threshold value is set. The Mahalanobis distance is calculated between the starting particles with the other particle that is illustrated as:

$$M_d = \left[(q_1(r), q_i(r))^T \, Cov^{-1} \, (q_1(r) - q_i(r))\right], \quad i = 2, 3, \dots, Z_p \tag{17}$$

Wherein, T implies the transposed of the position of the initial particle along with the remaining particle, M_d signifies the computed distance and Cov^{-1} implies the inverse covariance matrix. If the attained distance exceeds the fixed threshold value for the exact particle position, that particle is mutated. Next, the velocity along with the position is updated. The optimum progress is the requisite to move the particle position to ameliorate the objective function's value.

The velocity together with position updation of the particle is evinced as:

$$H_i(r + 1) = \varphi H_i(r) + A_1 \lambda_1 (L_i - Q_i(r)) + A_2 \lambda_2 (O - Q_i(r)) \tag{18}$$

$$Q_i(r + 1) = Q_i(r) + H_i(r + 1) \tag{19}$$

Wherein, A_1 and A_2 implies the '2' acceleration constants, termed as cognitive and social parameters, correspondingly, O signifies the best position of the particle found presently, λ_1 and λ_2 are the two random functions in the gamut [0,1], φ signifies the inertia weight, $Q_i(r)$ ascertained the position vector of particle i in r time, $H_i(r)$ implies the velocity vector of particle i in r time, and L_i signifies the personal best solution of particle i. By utilizing this PIDC with MPSO, FA is controlled and the SSS is enhanced and thus SS error is reduced.

Fig. 3 displays the MPSO pseudo-code, that presents the initialization, mutation, the procedure of computing distance between the starting and the other particles, along with the velocity, as well as position updation steps.

Input: initial parameters, P_i, I_i, and D_i
Output: tuning parameters

Begin
    Initialize parameters P_i, I_i, and D_i, firing angle $\Delta\alpha_i(t)$, ITAE T_e, error $e(t)$, particle
    index i, and maximum iteration Z_t.
    Calculate pbest and gbest $p_t(i,r) = \underset{r=1,......,t}{\arg\ \min}\ [e(q_i(r))]$ and
$$g_t(r) = \underset{\substack{i=1,......,Z_p \\ r=1,......,r}}{\arg\ \min}\ [e(q_i(r))]$$
    While $(\varepsilon = 1, \varepsilon \leq Z_t, \varepsilon++)$ **do**
        for each particle **do**
            Evaluate fitness function $T_e = \int_0^\infty (t.|e(t)|).dt$
            if $(T_e > p_t(i,r))$ {
                $p_t(i,r) = H_i(r)$
            }
            end if
        end for
        $g_t(r) = p_t(i,r)$ in $H_i(r)$
        Mutate the position of the particle by using Mahalanobis distance M_d
        for each particle **do**
            Calculate particle velocity $H_i(r+1)$
            Update particle position $Q_i(r+1)$
        end for
        Return optimal parameters
    End while
End

Figure 3: Pseudo code for the proposed MPSO

4 Result and Discussions

This section presents the proposed SSS enhancement system and its performance. For the purpose of simulation, MATLAB/SIMULINK platform is utilized. Fig. 4 shows the simulation model of the proposed SSS enhancement system,
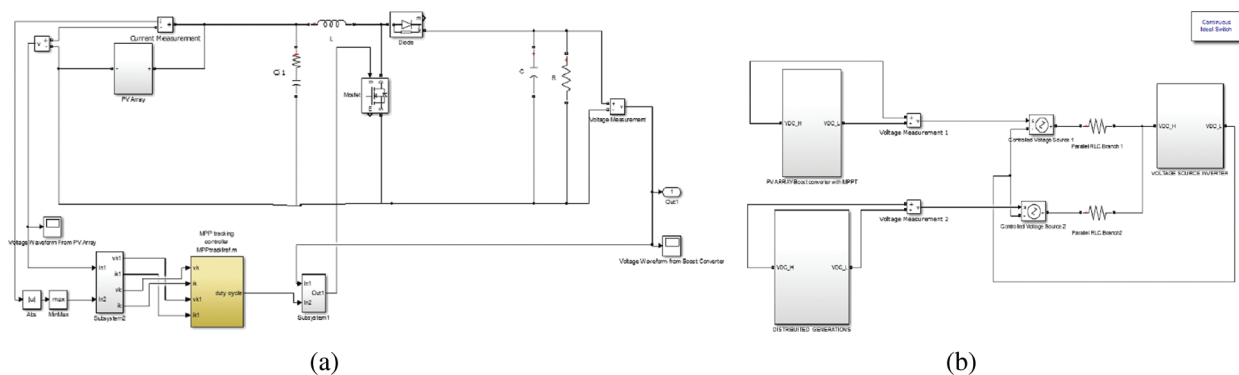

(a)   (b)

Figure 4: Matlab simulation of (a) PV array with MPPT and BC, and (b) Hybrid MG

Fig. 4 shows the Simulink output of (a) the PVA with MPPT and BC and (b) the hybrid MG design. In Fig. 4a, the BC is employed for realizing the MPPT operation and acquiring the DC voltage output. By effectuating MPPT, the working voltage shifts closest to the utmost extreme power under different weather conditions, and thereby ameliorates the hybrid PS's efficiency. The MPPT creates the control signal, which feeds the BC. The BC endeavors to elevate the output voltage level. This BC converts DC to AC current. Fig. 4b elucidates the voltage source inverter in detail. The voltage sources as of the distributed generator and the PVA BC with MPPT is strictly regulated by voltage source controllers.

4.1 Performance Analysis

Here, the proposed work is examined based on the performance, in respect of obtained current and voltage waveforms. The analyses could be explicated further using the below figures.

Fig. 5 shows the output of the PVA with a BC utilizing incremental conductance MPPT. The output voltage is analyzed in respect of time in seconds. MPPT boost provides 1200 V output voltage in 0.12 s time, 400 V in 0.05 s, and, 1130 V in 0.1 s. For the remaining time duration (*i.e.*, 0.15 s, 0.2 s, 0.25 s, and 0.3), 1200 V output is gained as of the MPPT boost. After 0.12 s, the maximal voltage is acquired. On this account, it elucidates that, the acquired voltage level is 1200 V for the MPPT BC, as of PVA.
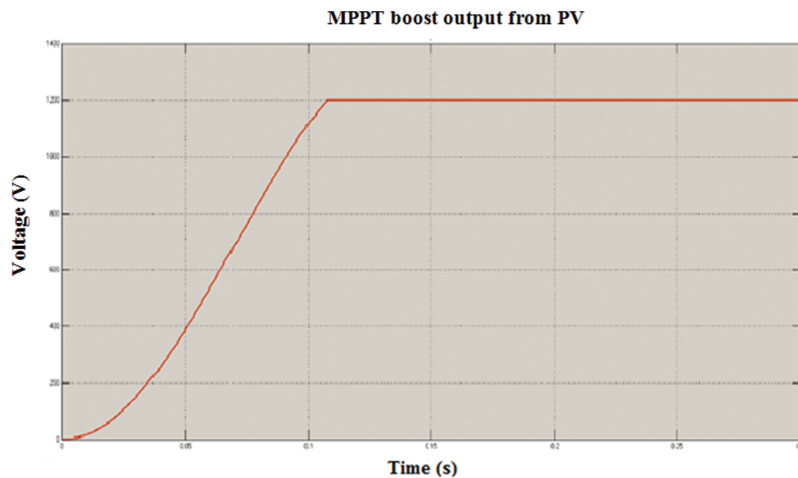

Figure 5: Output analysis of MPPT boost from PV array

Fig. 6 shows the voltage waveform as of the PVA. The analysis is made by means of varying the time between the generation and voltage. This analysis shows that a constant voltage of 694.5 V in entire time variation is noticed.

Fig. 7 shows the simulated outcomes of the voltage as well as current waveform of the implemented work. In 0.02 s, the current waveform varies as of −1 Kw to 1 Kw as shown in the top, followed by −5 Kw to 5 Kw in the second. Next, the third, fourth, and fifth simulated outcomes show the voltage waveforms. In between the time intervals, the voltage ventures into the negative value for the first three time-interval and it has a positive value for the other three time-interval.

Fig. 8 shows the distribution grid voltage profile. Here, the voltage varies between −200 V to 200 V. The simulated outcomes of the distribution grid voltage profile are analyzed based on time in seconds. Here, the attained voltage is the same as of 0.05 s to 0.3 s.
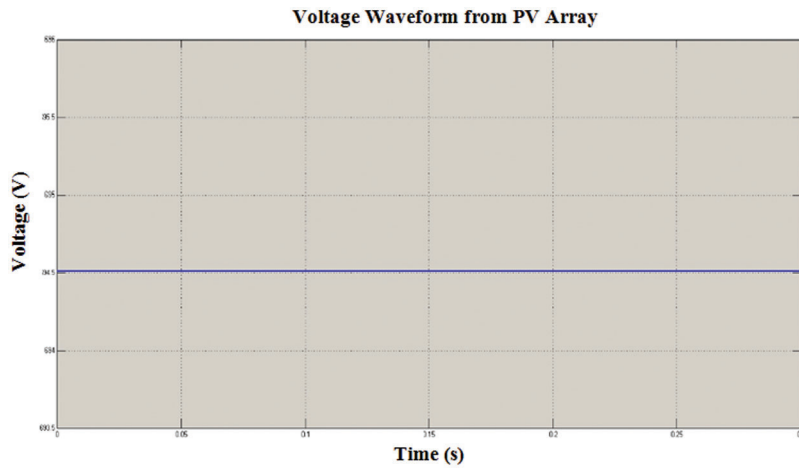
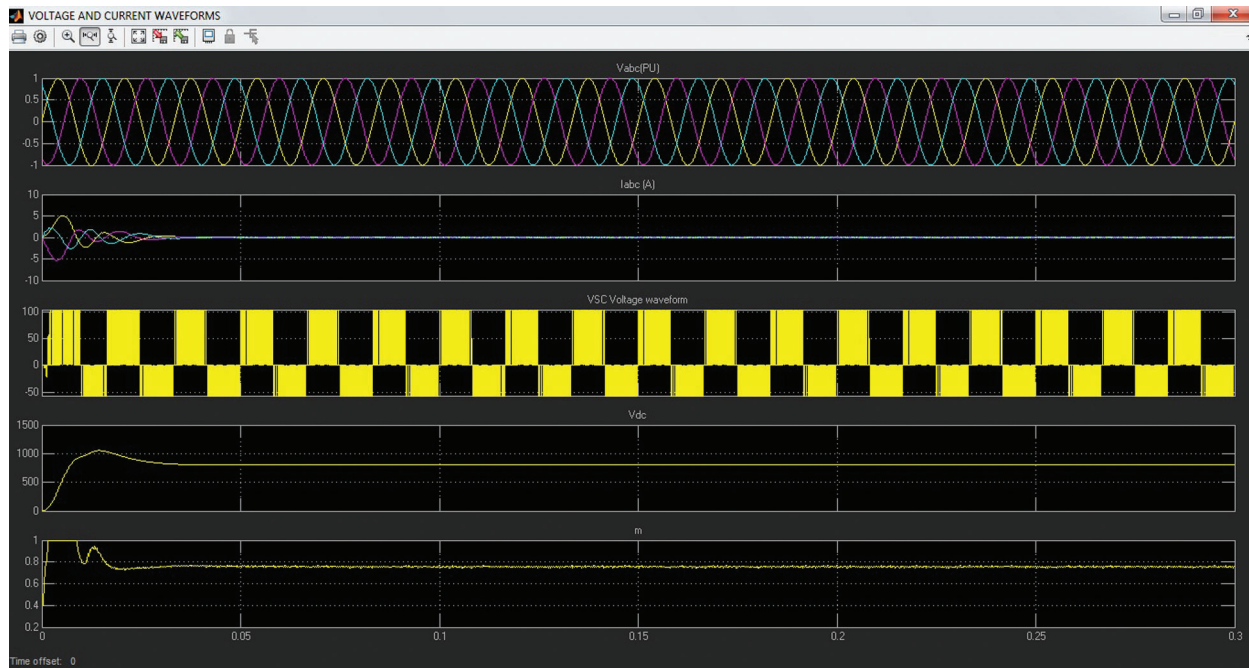**Figure 6:** Analysis of voltage waveform from PV array

Figure 7: Simulated result of voltage and current waveforms

Fig. 9 displays the simulated graph of the reference signal (RS) for gate pulse generation. The RS is utilized for testing the system capability. Here, the PIDC signal, the optimal parameter selection regarding an objective function in MPSO, and the signal acquired after velocity updation utilizing MPSO are shown. Subsequent to updating, the signal has an excellent result, and the performance is given.

4.2 Comparative Analysis

The Proposed MPSO is compared to the existing PSO [21], FF-PSO [23], DGA-BFA [24], and GA [20] based on fitness performance. This comparison have been performed for different iterations. Tab. 1 shows the fitness values attained by different algorithms,
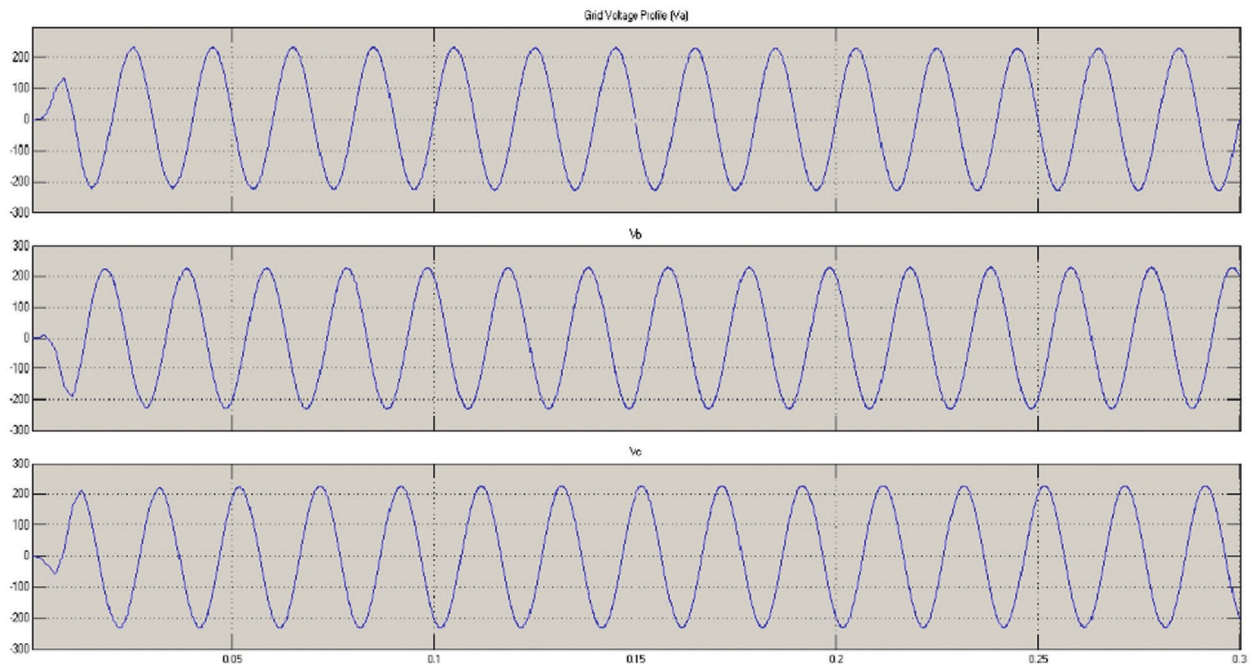
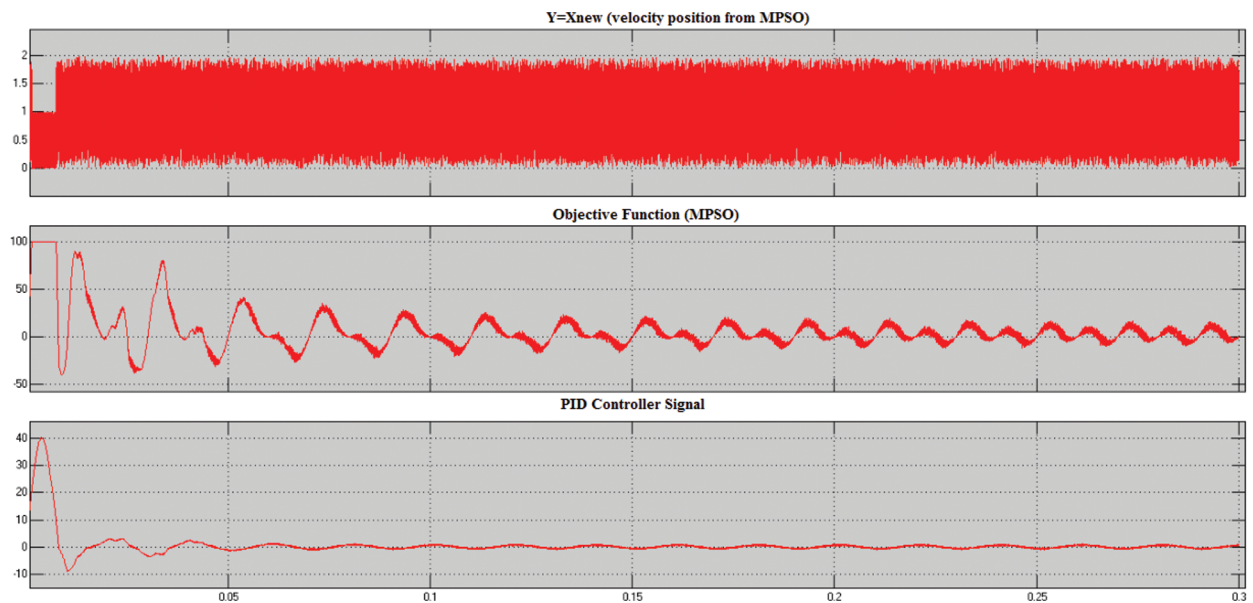**Figure 8:** Distribution grid voltage profile

Figure 9: Simulated result of reference signals for gate pulse generation

Tab. 1 shows the FF attained by the proposed MPSO algorithm and the existing FF-PSO, PSO, DGA-BFA, and GA algorithm, in respect of iterations (10 to 50). For 50 iterations, the MPSO algorithm attained 0.961- FF, whereas, the existing PSO has 0.876, existing FF-PSO has 0.899, DGA-BFA has 0.860 and the existing GA has 0.832 FF. Moreover, the proposed MPSO acquires the highest FF whilst the existing GA achieves the lower-most FF. FF-PSO, PSO, DGA-BFA is much better as compared to GA. Likewise, for the remaining iterations, the proposed method has better fitness results than the existing ones. From this analysis, the proposed work

based optimal parameter selection is confirmed to achieve a better result, as confirmed to the existing algorithms. The graphical explanation of fitness *vs.* iteration analysis is plotted in Fig. 10,

Table 1: Fitness *vs.* iteration analysis

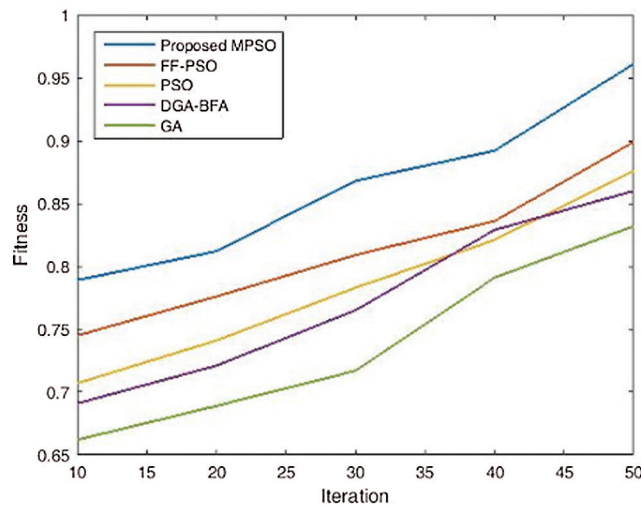| Iteration	Proposed MPSO	FF-PSO [23]	PSO [21]	DGA-BFA [24]	GA [20]
10	0.789	0.745	0.707	0.691	0.662
20	0.812	0.776	0.741	0.721	0.689
30	0.868	0.809	0.783	0.765	0.717
40	0.892	0.836	0.821	0.829	0.791
50	0.961	0.899	0.876	0.860	0.832

Figure 10: Graphical representation of fitness *vs.* iteration analysis

5 Conclusion

As SSS has an imperative role in ensuring the proper functioning of an MG system, SSS enhancement is requisite. The instability issues may arise, on account of the unsuitable parameters in the controller, which might affect the SSS. PIDC with the MPSO algorithm in DC-AC hybrid MG is proposed in this research for enhancing the SSS. Initially, the power is derived from the combination of RER. Here, excessive power is stored in a battery. Next, the converters and their controllers are explicated. Amid the experimentation investigation, the performance shown by means of the proposed system is analyzed based on the current and voltage waveforms, where better current and voltage are obtained with proposed one. Also, the RS for the pulse generation is analyzed. Then, the MPSO is compared to the existing PSO, FF-PSO, DGA-BFA, and GA, in respect of their fitness values. The MPSO acquired the higher most fitness value. Henceforth, the proposed work is perceived to attain SSS enhancement. In the future, the proposed work can well be extended by utilizing advanced controller approaches, and more RER are joined to acquire high power.

Conflicts of Interest: The authors declare that they have no conflicts of interest to report regarding the present study.

References

[1] Z. Li and M. Shahidehpour, "Small-signal modeling and stability analysis of hybrid ac/dc microgrids," *IEEE Transactions on Smart Grid*, vol. 10, no. 2, pp. 1–11, 2018.

[2] A. Ali, W. Li, R. Hussain, X. He, B. W. Williams *et al.,* "Overview of current microgrid policies, incentives and barriers in the European Union, United States and China," *Sustainability*, vol. 9, no. 7, pp. 1146, 2017.

[3] Y. Zhang, Q. Sun, J. Zhou, L. Li, W. Panfeng *et al.,* "Coordinated control of networked AC/DC microgrids with adaptive virtual inertia and governor-gain for stability enhancement," *IEEE Transactions on Energy Conversion*, vol. 36, no. 1, pp. 1–11, 2020.

[4] D. K. Dheer, S. Doolla and A. K. Rathore, "Small signal modeling and stability analysis of a droop based hybrid AC/DC microgrid," in *Proc. IES*, Florence, Italy, IEEE, pp. 3775–3780, 2016.

[5] B. Xie, Y. Liu, Y. Ji and J. Wang, "Two-stage battery energy storage system (BESS) in AC microgrids with balanced state-of-charge and guaranteed small-signal stability," *Energies*, vol. 11, no. 2, pp. 322, 2018.

[6] A. U. Krismanto, N. Mithulananthan and A. Lomi, "Dynamic droop control in microgrid for stability enhancement considering RES variation," in *Proc. ISGT*, Europe, pp. 1–6, 2017.

[7] S. Parhizi, H. Lotfi, A. Khodaei and S. Bahramirad, "State of the art in research on microgrids: A review," *IEEE Access*, vol. 3, pp. 890–925, 2015.

[8] H. R. Baghaee, M. Mirsalim, G. B. Gharehpetian and H. A. Talebi, "A decentralized power management and sliding mode control strategy for hybrid AC/DC microgrids including renewable energy resources," *IEEE Transactions on Industrial Informatics*, vol. 3, pp. 1–11, 2017.

[9] Y. Yan, D. Shi, D. Bian, B. Huang, Z. Yi *et al.,* "Small-signal stability analysis and performance evaluation of microgrids under distributed control," *IEEE Transactions on Smart Grid*, vol. 10, no. 5, pp. 4848–4858, 2019.

[10] R. Majumder, "Some aspects of stability in microgrids," *IEEE Transactions on Power Systems*, vol. 28, no. 3, pp. 3243–3252, 2013.

[11] B. Wen, D. Boroyevich, R. Burgos, P. Mattavelli and Z. Shen, "Small-signal stability analysis of three-phase AC systems in the presence of constant power loads based on measured d-q frame impedance," *IEEE Transactions on Power Electronics*, vol. 30, no. 10, pp. 5952–5963, 2015.

[12] A. Aderibole, H. H. Zeineldin, M. S. E. Moursi, J. C. H. Peng and M. A. Hosani, "Domain of stability characterization for hybrid microgrids considering different power sharing condition.0s," *IEEE Transactions on Energy Conversion*, vol. 33, no. 1, pp. 312–323, 2018.

[13] F. S. Rahman, T. Kerdphol, M. Watanabe and Y. Mitani, "Active power allocation of virtual synchronous generator using particle swarm optimization approach," *Energy and Power Engineering*, vol. 09, no. 04, pp. 414–424, 2017.

[14] A. Karimi, Y. Khayat, M. Naderi, R. Mirzaee and H. B. Evrani, "Improving transient performance of VSG based microgrids by virtual FACTS functions," in *Proc. SGC*, Tehran, Iran, 2018.

[15] A. Khodadadi, P. H. Divshali, M. H. Nazari and S. H. Hosseinian, "Small-signal stability improvement of an islanded microgrid with electronically-interfaced distributed energy resources in the presence of parametric uncertainties," *Electric Power Systems Research*, vol. 160, no. 9, pp. 151–162, 2018.

[16] A. Mohanty, M. Viswavandya, D. Mishra, P. K. Ray, S. Patra *et al.,* "An optimized STATCOM controller for voltage stability and reactive power compensation in an isolated microgrid," in *Proc. PCITC*, Bhubaneswar, India, 2015.

[17] H. Moussa, A. Shahin, J. P. Martin, S. Pierfederici and N. Moubayed, "Optimal angle droop for power sharing enhancement with stability improvement in islanded microgrids," *IEEE Transactions on Smart Grid*, vol. 9, no. 5, pp. 5014–5026, 2018.

[18] P. C. Sekhar, S. Mishra and R. Sharma, "Data analytics based neuro-fuzzy controller for diesel-photovoltaic hybrid AC microgrid," *IET Generation, Transmission & Distribution*, vol. 9, no. 2, pp. 193–207, 2015.

[19] P. Satapathy, S. Dhar and P. K. Dash, "Stability improvement of PV-BESS diesel generator-based microgrid with a new modified harmony search-based hybrid firefly algorithm," *IET Renewable Power Generation*, vol. 11, no. 5, pp. 566–577, 2017.

[20] M. Regad, M. Helaimi, R. Taleb, H. A. Gabbar and M. A. Othman, "Fractional order PID control of hybrid power system with renewable generation using genetic algorithm," in *Proc. SEGE*, IEEE, pp. 139–144, 2019.

[21] M. Regad, M. Helaimi, R. Taleb, A. M. Othman and H. A. Gabbar, "Frequency control in microgrid power system with renewable power generation using PID controller based on particle swarm optimization," in *Proc. ICAIRES*, Cham, Springer, pp. 3–13, 2019.

[22] H. Shahsavari and A. Nateghi, "Optimal design of probabilistically robust controller to improve small signal stability of PV integrated power system," *Journal of the Franklin Institute*, vol. 356, no. 13, pp. 7183–7209, 2019.

[23] P. K. Ray and A. Mohanty, "A robust firefly-swarm hybrid optimization for frequency control in wind/PV/FC based microgrid," *Applied Soft Computing*, vol. 30, pp. 105823 (1–32), 2019.

[24] K. H. Abdulkhader, J. Jacob and A. Mathew, "Robust type-2 fuzzy fractional order PID controller for dynamic stability enhancement of power system having RES based microgrid penetration," *Int. Journal of Electrical Power & Energy Systems*, vol. 110, pp. 357–371, 2019.

[25] M. A. Nezhadpashaki, F. Karbalaei and S. Abbasi, "Optimal placement and sizing of distributed generation with small signal stability constraint," *Sustainable Energy, Grids and Networks*, vol. 80, pp. 100380 (1–9), 2020.

[26] S. M. M. Tafreshi, H. A. Zamani and S. M. Hakimi, "Optimal sizing of distributed resources in microgrid with loss of power supply probability technology by using breeding particle swarm optimization," *Journal of Renewable and Sustainable Energy*, vol. 3, no. 4, pp. 043105 (1–17), 2011.

[27] T. K. Renuka, P. Reji and S. Sreedharan, "An enhanced particle swarm optimization algorithm for improving the renewable energy penetration and small signal stability in power system," *Renewables: Wind, Water, and Solar*, vol. 5, no. 1, pp. 156, 2018.

[28] T. Santhoshkumar and V. Senthilkumar, "Transient and small signal stability improvement in microgrid using AWOALO with virtual synchronous generator control scheme," *ISA Transactions*, vol. 104, pp. 56–60, 2020.

[29] Y. Zhang, Q. Sun, J. Zhou, L. Li, W. Panfeng *et al.,* "Coordinated control of networked AC/DC microgrids with adaptive virtual inertia and governor-gain for stability enhancement," *IEEE Transactions on Energy Conversion*, vol. 36, no. 1, pp. 95–110, 2021.

[30] S. Ferahtia, A. Djerioui, S. Zeghlache and A. Houari, "A hybrid power system based on fuel cell, photovoltaic source and super capacitor," *SN Applied Sciences*, vol. 2, no. 5, pp. 1–11, 2020.

[31] S. Ramadoni and I. Soesanti, "Planning of hybrid micro-hydro and solar photovoltaic systems for rural areas of central java," *Indonesia Journal of Electrical and Computer Engineering*, vol. 2020, pp. 1–6, 2020.